CD11b+ Gr1+ Bone Marrow Cells Ameliorate Liver Fibrosis by Producing Interleukin-10 in Mice

Yang-Gun Suh[1], **Ja Kyung Kim**[2], **Jin-Seok Byun**[1], **Hyon-Seung Yi**[1], **Young-Sun Lee**[1], **Hyuk Soo Eun**[1], **So Yeon Kim**[1], **Kwang-Hyub Han**[2], **Kwan Sik Lee**[2], **Gregg Duester**[3], **Scott L. Friedman**[4], and **Won-Il Jeong**[1]

Yang-Gun Suh: mdsuh@kaist.ac.kr; Ja Kyung Kim: ceciliak@yuhs.ac; Jin-Seok Byun: byonsatto@kaist.ac.kr; Hyon-Seung Yi: jmpbooks@kaist.ac.kr; Young-Sun Lee: lys810@kaist.ac; Hyuk Soo Eun: liver@kaist.ac.kr; So Yeon Kim: soyeon0121@kaist.ac.kr; Kwang-Hyub Han: gihankhys@yuhs.ac; Kwan Sik Lee: leeks519@yuhs.ac; Gregg Duester: duester@burnham.org; Scott L. Friedman: Scott.Friedman@mssm.edu; Won-Il Jeong: wijeong@kaist.ac.kr

[1]Graduate School of Medical Science and Engineering, Korea Advanced Institute of Science and Technology, Daejeon, Korea

[2]Department of Internal Medicine, Yonsei University College of Medicine, Seoul, Korea

[3]Sanford-Burnham Medical Research Institute, La Jolla, CA, USA

[4]Division of Liver Diseases, Mount Sinai School of Medicine, New York, New York, USA

Abstract

Clinical trials and animal models suggest that infusion of bone marrow cells (BMC) is effective therapy for liver fibrosis, but the underlying mechanisms are obscure, especially those associated with early effects of BMC. Here, we analyzed the early impact of BMC infusion and identified the subsets of BMC showing antifibrotic effects in mice with carbon tetrachloride-induced liver fibrosis. An interaction between BMC and activated hepatic stellate cells (HSCs) was investigated using *in vitro* co-culturing system. Within 24 hours, infused BMC were in close contact with activated HSCs, which was associated with reduced liver fibrosis, enhanced hepatic expression of interleukin (IL)-10, expanded regulatory T cells but decreased macrophage infiltration in the liver at 24 hours after BMC infusion. In contrast, IL-10-deficient (IL-10$^{-/-}$) BMC failed to reproduce these effects in the fibrotic livers. Intriguingly, in isolated cells, CD11b$^+$Gr1^{high}F4/80$^-$ and CD11b$^+$Gr1$^+$F4/80$^+$ BMC expressed more IL-10 after co-culturing with activated HSCs, leading to suppressed expression of collagen and a-smooth muscle actin in HSCs. Moreover, these effects were either enhanced or abrogated, respectively, when BMC were co-cultured with IL-6$^{-/-}$ and retinaldehyde dehydrogenase 1$^{-/-}$ HSCs. Similar to murine data, human BMC expressed more IL-10 after co-culturing with human HSC lines (LX-2 or hTERT), and serum IL-10 levels were significantly elevated in patients with liver cirrhosis after autologous BMC infusion.

Conclusion—Activated HSCs increase IL-10 expression in BMC (CD11b$^+$Gr1^{high}F4/80$^-$ and CD11b$^+$Gr1$^+$F4/80$^+$ cells), which in turn ameliorates liver fibrosis. Our findings could enhance the design of BMC therapy for liver fibrosis.

Keywords

hepatic stellate cell; interleukin-6; regulatory T cell; retinoic acid

For the past decade, clinical trials and experimental studies have suggested that infusion therapy of whole bone marrow cells (BMC) has beneficial effects towards liver

Contact information: Won-Il Jeong, DVM, Ph.D, Laboratory of Liver Research, Bldg E7 Rm8107, GSMSE/KAIST, 373-1 Guseong-dong, Yuseong-gu, Daejeon 305-701, Korea Tel: 82-42-350-4239; wijeong@kaist.ac.kr.

regeneration, injury and fibrosis/cirrhosis by stimulating the proliferation of hepatocytes, increasing progenitor cells and enhancing matrix degradation.[1–3] However, the underlying mechanisms are unknown, in part because whole BMC contain a wide range of cell types including several types of stem and precursor cells of monocytic and granulocytic lineages.[4] Events associated with hepatic fibrosis are well characterized, notably the excessive production of extracellular matrix (ECM) by activated hepatic stellate cells (HSCs).[5] Activated HSCs produce not only huge amounts of ECMs including collagen, but also other fibrosis-related mediators including transforming growth factor (TGF)-β1, interleukin (IL)-6, IL-10 and retinoic acid.[5–7] Interestingly, treatments with TGF-β1, IL-6 and retinoic acid can differentiate naïve T cells into regulatory T cells (Tregs) or Th-17 cells *in vitro*, in which TGF-β1 is considered as an initial driver of this commitment.[8] Moreover, activated HSCs produce these mediators, implicating activated HSCs in immune regulation.

Recent studies underscore this immunoregulatory potential of HSCs, wherein they can act as intrahepatic antigen presenting cells to activate T, natural killer (NK), and NKT cells[9, 10] and are also involved in the induction of $CD11b^+Gr1^+$ myeloid-derived suppressor cells (MDSCs) and $CD4^+CD25^+Foxp3^+$ Tregs in an interferon (IFN)-γ and retinoic acid-dependent manner, respectively.[11, 12] MDSCs expressing both markers of CD11b and Gr1 are now appreciated as a negative regulator of immune responses in cancer and other diseases. In addition, MDSCs are closely related to the induction of Tregs in the tumor microenvironment, which could produce IL-10 through the activity of the transcription factor, Foxp3.[13–15] Moreover, IL-10 is recognized as an anti-inflammatory and anti-fibrotic mediator.[5, 6] These findings provide a rationale for the possible immunoregulatory role of HSCs *in vivo* during BMC infusion therapy. In fact, infused BMC have been detected in fibrotic areas within 24 hours and can replace 25% of recipient hepatocytes by 4 weeks.[16] However, the mechanisms underlying the effects of BMC are still uncertain, and most studies of infused BMC therapy have focused on hepatocyte regeneration and ECM degradation as long-term effects of BMC (at least 2 week after BMC infusion) in liver fibrosis.[1, 2] Contrary to these previous findings, in the current study, we show that HSCs directly interact with infused BMC, especially $CD11b^+Gr1^{high}F4/80^-$ and $CD11b^+Gr1^+F4/80^+$ cells among whole BMC isolates at an early phase *in vivo* (within 24 hours). This interaction drives production of IL-10 in both types of cells, leading to increased Tregs in the recipient liver, which attenuates fibrosis.

Materials and Methods

Animals

Male C57BL/6, $IL-6^{-/-}$, $IL-10^{-/-}$ and green fluorescence protein (GFP)-transgenic mice were purchased from The Jackson Laboratory (Bar Harbor, ME). B6/SJL (CD45.1) mice were purchased from Taconic (Germantown, NY, USA). Retinaldehyde dehydrogenase 1 $(RALDH1)^{-/-}$ mice (backcrossed to the B6 strain for more than 9 generation) were friendly obtained from Dr. Gregg Duester (Sanford-Burnham Medical Research Institute, CA, USA). The mice were bred in the specific pathogen-free facility, Bio Model System Park (KAIST, Daejeon, Korea). All animal experiments were approved by KAIST Institutional Animal Care and Use Committee. To induce liver fibrosis, 8- to 10-week-old mice were treated with 0.4 ml/Kg carbon tetrachloride (CCl_4) diluted in olive oil via intraperitoneal injection 3 times per week for 2 weeks. Twenty-four hours after the last injection of CCl_4, 1×10^6 whole BMC or control medium were transferred to mice via tail vein. Twelve or 24 hours after infusion of BMC, mice were sacrificed.

Patients (human study population)

Human BMC were harvested from patients with HBV-induced liver cirrhosis for autologous BMC infusion in Severance Hospital (Seoul, Korea). Some BMC were used for *in vitro* experiments with the patients' consent. Serum data were obtained from patients treated with autologous BMC infusion between November 2006 and February 2008. The protocol for the clinical trial conformed to the ethical guidelines of the Declaration of Helsinki and was approved by the Institutional Review Board of Severance Hospital in the Yonsei University Health System.

Statistical Analysis

Data were expressed as mean ± standard error of the mean (SEM). To compare values, the Student's *t* test or ANOVA was performed. For blood samples of patients, Wilcoxon's signed-ranks test with Bonferroni correction was used to compare the values of paired samples. A value of $P < 0.05$ was considered statistically significant.

All other materials and methods are described in the Supporting Information.

Results

Infused BMC ameliorates CCl₄-induced liver fibrosis in mice

To investigate early events following infusion of BMC in fibrotic liver, mice with CCl_4-induced liver fibrosis were sacrificed at 12 and 24 hours after infusion with BMC from GFP^+ mice via tail vein. At 12 and 24 hours, serum levels of ALT, AST, triglyceride, albumin, cholesterol and glucose were not changed compared with those of vehicle-infused mice (Fig. 1A and Supporting Fig. 1A). However, collagen fibers and α-smooth muscle actin (SMA) positive HSCs in liver tissues of BMC-infused mice were decreased compared to those of vehicle-infused mice at 12 and 24 hours (Fig. 1B and Supporting Fig. 1B), which were confirmed by Western blotting (Fig. 1C) and quantitative RT-PCR (qRT-PCR) analyses (Fig. 1D) in isolated HSCs. In contrast, relative mRNA levels in HSCs for TGF-β1, IL-6 and monocyte chemoattractant protein (MCP)-1 were decreased only at 24 hours in BMC-infused mice but not in vehicle-infused mice, whereas there was no significant difference in IL-10 mRNA expression in HSCs (Supporting Fig. 1C). More surprisingly, most of migrated GFP^+ BMC were in close contact with activated HSCs in the fibrotic septa within 24 hours (Fig. 1E and Supporting Fig. 1D). These results suggested that migrated BMC might influence collagen production by activated HSCs via direct cell-cell interaction.

Infused BMC increase IL-10 expression and CD4⁺CD25⁺Foxp3⁺ Tregs while decreasing the expression of IL-6 and MCP-1, and reducing CD11b⁺F4/80⁺ cells in fibrotic liver

We next examined the changes of inflammatory mediators and cells in the liver after infusion of BMC. Isolated liver mononuclear cells (MNCs) of BMC-infused mice had higher expression of IL-10 and Foxp3, but reduced expression of pro-inflammatory MCP-1 and IL-6 compared to vehicle-infused mice (Fig. 2A). Since Foxp3 is a master regulator of Tregs that induces production of IL-10, we analyzed intrahepatic frequencies of Tregs by fluorescence-activated cell sorting (FACS) analyses (Supporting Fig. 2A). By gating for liver lymphocytes, mice with infused BMC displayed a significant increase in $CD4^+CD25^+Foxp3^+$ Tregs compared with that of vehicle-infused mice, and the increased Tregs did not express GFP, suggesting that they were derived from recipient mice (Fig. 2B and Supporting Fig. 2B).

As the anti-inflammatory effects of Tregs are attributable to IL-10 and TGF-β1, we assessed the intrahepatic infiltration of $CD11b^+F4/80^+$ macrophages, $NK1.1^+CD3^-$ NK cells and $Gr1^+CD11b^+$ granulocytes. While the numbers of NK cells and granulocytes were not

affected by infusion of BMC (Supporting Fig. 2C), CD11b$^+$F4/80$^+$ macrophages were significantly decreased at 24 hours after BMC infusion compared with those of vehicle-infused mice (Fig. 2C and Supporting Fig. 2D). In addition, many of GFP$^+$ BMC were observed in the regions where there were decreased numbers of CD11b$^+$F4/80$^+$ cells (Supporting Fig. 2D). Some of the infused BMC were double-positive for GFP (green) and F4/80 (red) in the inflammatory regions (Supporting Fig. 2E). Because TGF-β1 is not only an important driver of liver fibrosis but also a major cytokine of Tregs, macrophage and HSCs, we assayed TGF-β1 expression in whole liver tissues, isolated HSCs and liver MNCs. TGF-β1 expression in whole liver tissues and isolated HSCs was ameliorated in BMC-infused mice compared with those of vehicle-infused mice at 24 hours (Fig. 2D and Supporting Fig. 1C). In contrast, TGF-β1 expression in liver MNCs was significantly increased at 12 hours whereas there was no difference at 24 hours in BMC-infused compared to vehicle-infused mice (Fig. 2E).

Infused BMC subtypes CD11b$^+$Gr1^{high}F4/80$^-$ and CD11b$^+$Gr1$^+$F4/80$^+$ produce IL-10 in fibrotic livers of recipient mice

Similar to a previous report,[16] approximately 0.3% of liver MNCs in recipient mice were comprised of GFP$^+$ BMC at 12 and 24 hours after BMC infusion (Fig. 3A). Moreover, less than 0.1% and 0.6–1.0% GFP$^+$ cells were identified in gates of lymphocytes and monocyte/granulocytes, respectively (Fig. 3A). Furthermore, in analyzing infused BMC in fibrotic liver, almost all GFP$^+$ cells had originated from bone marrow-derived hematopoietic cells (CD45 positive), and most of them (75–80%) expressed CD11b and Gr1 (Supporting Fig. 3A), which are specific markers for the myeloid-cell lineage differentiation.[4, 17] Thus, we analyzed GFP$^+$ BMC using antibodies to Gr1 and F4/80 to distinguish between granulocyte and monocyte lineages. Around 75% of GFP$^+$ BMC were positive for Gr1, whereas 20% of them expressed F4/80 (Fig. 3B). Next, we investigated subsets of infused BMC using antibodies to CD11b, Gr1 and F4/80 after gating with CD45. Most of the GFP$^+$ BMC (~80%) were double-positive for Gr1 and CD11b and, after gating with CD45 and CD11b, CD11b$^+$Gr1^{high}F4/80$^-$, CD11b$^+$Gr1^{low}F4/80$^-$ and CD11b$^+$Gr1$^+$F4/80$^+$ cells comprised about 25%, 16% and 15% of infused GFP$^+$ BMC, respectively (Supporting Fig. 3). More surprisingly, IL-10 positive infused BMC were identified as CD11b$^+$Gr1$^+$ cells, which could be further subdivided into CD11b$^+$Gr1^{high}F4/80$^-$, and CD11b$^+$Gr1$^+$F4/80$^+$ cells (Fig. 3C, D). Thus, IL-10$^+$CD11b$^+$Gr1$^+$F4/80$^+$ and IL-10$^+$CD11b$^+$Gr1^{high}F4/80$^-$ BMC appear to be undifferentiated cells that might belong to the monocytic and granulocytic lineages, respectively, based on their morphology, cytoplasmic granules and CD markers (Fig. 3C-E).

Co-culturing with HSCs enhances IL-10 expression by BMC, which suppresses expression of α-SMA and Col1a1 in HSCs

Because infused BMC in fibrotic area were adjacent to activated HSCs and displayed increased IL-10 expression (Fig. 1E and 3C), we hypothesized that enhanced IL-10 expression in infused BMC might be due to their interactions with HSCs. To test this hypothesis, we co-cultured BMC with activated HSCs up to 24 hours (Fig. 4A and Supporting Fig. 4A). IL-10 expression in adherent and floating BMC significantly increased after co-culturing, but floating BMC expressed higher IL-10 than adherent BMC at 6 hours (Fig. 4B and Supporting Fig. 4B). In contrast, expression of α-SMA and collagen 1A1 (COL1A1) genes in HSCs was significantly reduced by co-culturing with BMC (Fig. 4C).

Next, we examined whether IL-10 secretion from human BMC could be enhanced by co-culturing with human HSCs (Supporting Fig. 4C). Once human BMC stuck to HSCs, it was difficult to separate the two cell types; therefore, we collected only floating human BMC after co-culturing, and analyzed expression of IL-10. In qRT-PCR analyses, IL-10 expression was increased in human BMC co-cultured with LX-2 and hTERT HSC cell lines

at 6 and 12 hours (Fig. 4D). These data were concordant with those of mice. Therefore, we assessed the IL-10 levels in the sera of patients (n=15) with liver cirrhosis after autologous BMC infusion therapy. Patient information is described in Supporting Table 1. After autologous BMC infusion, a trend towards increased IL-10 was detected in the sera of patients, which was not statistically significant by Bonferroni correction (Fig. 4E). Then, we further analyzed IL-10 levels in patients. First, patients were separated into two groups as follows: After autologous BMC infusion, patients (n=10) with improved Child-Pugh scores and albumin levels were designated as the 'effective' group and patients (n=5) with no improvements were the 'non-effective' group. Surprisingly, patients in the effective group after autologous BMC infusion expressed significantly more IL-10 at day 1 (P=0.03027 by Bonferroni correction), which was sustained for 14 days (not significant), while patients in the non-effective group had no difference in IL-10 levels compared with those of day 0 (Fig. 4F and Supporting Fig. 4D). These data reinforce IL-10 as a potential factor in the early response to BMC infusion therapy for treatment of hepatic fibrosis in mice as well as humans.

CD11b$^+$Gr1^{high}F4/80$^-$ and CD11b$^+$Gr1$^+$F4/80$^+$ BMC enhance IL-10 expression after co-culturing with D4 HSCs

To further investigate IL-10 expression by BMC *in vitro*, we analyzed the subsets of BMC after co-culturing with HSCs. Since the major sources of IL-10 among infused BMC were identified as CD11b$^+$Gr1^{high}F4/80$^-$ and CD11b$^+$Gr1$^+$F4/80$^+$ cells *in vivo* (Fig. 3C), we investigated whether adherent and floating BMC contained both types of cells. In FACS analyses after co-culturing, adherent BMC contained a higher fraction of CD11b$^+$Gr1$^+$F4/80$^+$ cells (18%) than those of floating cells (6%), while the frequency of CD11b$^+$Gr1^{high}F4/80$^-$ cells (87%) in floating BMC exceeded that of adherent cells (50%) at 6 hours (Fig. 5A and Supporting Fig. 5A). After 6 hours of co-culture, IL-10 positive cells in adherent and floating BMC were higher than those of control BMC, respectively (Fig. 5B and Supporting Fig. 5B). Therefore, we further analyzed IL-10 positive cells of BMC using antibodies to CD11b, Gr1 and F4/80. After co-culturing with HSCs, the frequencies of CD11b$^+$IL-10$^+$ cells in adherent (8%) and floating (5%) BMC were much higher than those (4.7% and 1.8%) of control BMC; CD11b$^+$Gr1$^+$F4/80$^+$ cells and CD11b$^+$Gr1^{high}F4/80$^-$ cells were identified as major IL-10 producing cells in adherent and floating BMC, respectively (Fig. 5C,D and Supporting Fig. 5C). However, CD11b$^-$IL-10$^+$ cells in control and co-cultured BMC showed similar frequencies, which were mostly recognized as CD11b$^-$Gr1$^+$F4/80$^+$ cells (Supporting Fig. 5D).

To characterize the morphologies of IL-10 producing BMC, CD11b$^+$Gr1$^+$F4/80$^+$ and CD11b$^+$Gr1^{high}F4/80$^-$ cells were sorted and then stained with Giemsa followed by immunocytochemistry for IL-10. Using Giemsa staining, monocytic cells with vesicles (black arrow head) and granules (white arrow head) were the major types among the CD11b$^+$Gr1$^+$F4/80$^+$ adherent BMC, in which monocytic cells with non-indented nuclei (black arrow head) were positive for IL-10 (Fig. 5E, upper panels). In contrast, granulocytic cells (white arrow) and their precursor cells (black arrow) were the main cell types among CD11b$^+$Gr1^{high}F4/80$^-$ floating BMC, in which precursor type cells (black arrow) were positive for IL-10 (Fig. 5E, lower panels). In addition, further analyses of BMC with additional antibodies to Ly6G and Ly6C, the CD11b$^+$Gr1$^+$F4/80$^+$ and CD11b$^+$Gr1^{high}F4/80$^-$ cells were identified as CD11b$^+$Ly6G$^-$Ly6C^{high} and CD11b$^+$Ly6G$^+$Ly6C^{low} cells, respectively (Supporting Fig. 5E). Based on these findings, adherent and floating BMC expressing IL-10 might be monocytic and granulocytic MDSC-like cells, respectively. Other Gr1^{low}F4/80$^-$ BMC were identified as precursor cells for granulocytes and monocytes (Supporting Fig. 5F).

Infused BMC-derived IL-10 is a key molecule for ameliorating liver fibrosis and expansion of liver Treg

To confirm the antifibrotic role of infused BMC-derived IL-10 in liver fibrosis, we infused IL-10-deficient BMC to mice with CCl_4-induced liver fibrosis. As expected, Sirius red staining and immunohistochemistry for α-SMA demonstrated that liver fibrosis was significantly ameliorated in wild type (WT) BMC-infused mice but not in IL-10-deficient BMC-infused mice compared with the controls (Fig. 6A). Image analyses and Western blotting further confirmed these findings (Fig. 6B, C). qRT-PCR showed significantly increased IL-10 mRNA expression in liver MNCs of WT BMC-infused mice, but not in IL-10-deficient BMC-infused mice, compared with the controls (Fig. 6D). Moreover, frequencies of Tregs in livers of IL-10-deficient BMC-infused mice were unchanged compared with the controls (Fig. 6E, F). These data indicate that infused BMC-derived IL-10 is a key molecule that accounts for the anti-fibrotic activity observed in this model.

IL-10 expression in BMC is promoted or suppressed by retinoic acid and IL-6 of HSCs, respectively

Finally, we sought to identify mediators of HSCs that affected expression of IL-10 in BMC. Because HSCs can produce IL-6, IL-10 and RALDH1-mediated retinoic acid, these factors have been considered as candidate components driving the inflammatory reaction, and expansion and differentiation of Treg and MDSC.[11, 18–21] Accordingly, we co-cultured BMC with IL-6, IL-10 and RALDH1 gene-depleted HSCs, respectively. In the absence of IL-6 in HSCs, IL-10 expression was significantly increased in both adherent and floating BMC compared with those of WT BMC co-cultured with WT HSCs ($P < 0.05$), whereas RALDH1-deficient HSCs did not increase IL-10 expression by BMC compared with those of WT BMC co-cultured with WT HSCs (Fig. 7A, B). In addition, IL-10-deficient WT HSCs increased IL-10 expression similarly in both adherent and floating BMC compared with those of WT BMC co-cultured with WT HSCs (Fig. 7A, B). To reinforce the effect of retinoic acid on IL-10 production by infused BMC *in vivo*, we administrated CCl_4 to RALDH1-deficient mice for 2 weeks, and then these animals were infused with WT BMC. Twenty-four hours after infusion of BMC, fibrosis was not ameliorated (Fig. 7C and Supporting Fig. 6A). Based on FACS analyses, there were no significant changes in the frequencies of inflammatory cells, such as $CD11b^+F4/80^+$ macrophages and $CD11b^+Gr1^+$ granulocytes, and Treg cells as well in liver (Fig. 7D and Supporting Fig. 6B, C).

Discussion

The beneficial effects of BMC therapy have been investigated recently in mice and humans, yet underlying mechanisms have been overlooked, especially the early effects of BMC. In the present study, we identify early phase anti-fibrotic effects of infused BMC *in vivo* and *in vitro*, which reflect the interaction between HSCs and BMC within 24 hours. Mechanisms of liver fibrosis amelioration by infused BMC are summarized in Figure 7E.

Contrary to the previously reported long-term effects of BMC in fibrotic livers of mice and humans,[1–3] we have shown that at early time points, infused BMC ameliorates liver fibrosis without any change in liver injury, hepatocyte regeneration or albumin production (Fig. 1 and Supporting Fig. 1A), suggesting that there are no effects of bone marrow-derived stem cells within 24 hours after infusion. In addition, the involvement of BMC-derived myofibroblasts in collagen production appears to be negligible during liver fibrogenesis.[22] Instead, we found that infused GFP^+ BMC, mostly expressing CD11b and Gr1, migrated into fibrotic septa adjacent to activated HSCs (Fig. 1E and Supporting Fig. 3A), which might result from the expression of CCR2 and MCP-1 in BMC and HSCs respectively,[5, 23, 24] whereas isolated HSCs of liver after infusion of BMC have decreased expression of α-SMA,

COL1A1, TGF-β, IL-6 and MCP-1 genes compared with those of controls (Fig. 1D and Supporting Fig. 1C). These findings suggest that infused BMC interact with HSCs and suppress liver fibrosis by inhibiting their activation.

In the present study, the expression of IL-10 was significantly increased in liver MNC within 24 hours following infusion of BMC, and its antifibrotic effect was abrogated when IL-10-deficient BMC were infused instead. Moreover, IL-10 expression of BMC was enhanced by co-culturing with activated HSCs, whereas activation of HSCs was inversely related to IL-10 expression (Fig. 4B, C). These co-culture findings are especially informative for the following reasons. First, both adherent and floating BMCs contained $CD11b^+Gr1^+F4/80^+$ and $CD11b^+Gr1^{high}F4/80^-$ cells (Fig. 5A). Second, although both $CD11b^+Gr1^+F4/80^+$ and $CD11b^+Gr1^{high}F4/80^-$ cells were enriched in adherent BMC and floating BMC respectively, these distributions changed over time. For instance, the population of $CD11b^+Gr1^{high}F4/80^-$ cells in floating BMCs decreased slowly after co-culturing, whereas their representation within adherent BMCs increased, and then a similar fraction was detected in adherent and floating BMC at 24 hour (Supporting Fig. 5A, left panel). Moreover, the population of $CD11b^+Gr1^+F4/80^+$ cells in adherent BMC slowly decreased and then approximated those of floating BMC at 24 hour after co-culturing with HSCs (Supporting Fig. 5A, right panel). Therefore, it is unclear whether there are differences between the adherent and non-adherent BMC based on the co-culture experiments. Further studies will be needed to resolve this question. In parallel to the murine data, enhanced expression and production of IL-10 were confirmed within 24 hours of co-culturing human BMC with human HSC lines (Fig. 4D), and in sera of human patients. respectively, consistent with beneficial effects following autologous BMC infusion (Fig. 4F). These findings indicate that BMC production of IL-10 is not only a critical event at an early phase after infusion of BMC, but is also a crucial negative regulator of liver fibrosis, as reported previously.[5, 6] Indeed, the source of IL-10 is primarily from infused BMC, especially $CD11b^+Gr1^{high}F4/80^-$ and $CD11b^+Gr1^+F4/80^+$ cells (Fig. 3C), and these cells were also identified as $CD11b^+Ly6G^+Ly6C^{low}$ and $CD11b^+Ly6G^-Ly6C^{high}$ cells respectively (Supporting Fig. 5E).

Based on prior reports, MDSCs are a heterogeneous population of immature cells capable of inhibiting immune responses, and were originally characterized based on their co-expression of the myeloid-cell lineage differentiation marker Gr1 and CD11b.[12, 17, 20] To date, MDSCs are distinguished between two subsets: granulocytic MDSCs have a $CD11b^+Ly6G^+Ly6C^{low}$ phenotype, whereas monocytic MDSCs have a $CD11b^+Ly6G^-Ly6C^{high}$ phenotype.[17] Thus, $IL-10^+$ BMC detected in recipient mice share the same markers with MDSC, as specific cells with a non-lobulated nucleus that produce IL-10 (Figs. 3E and 5E). Moreover, recent studies demonstrate that HSCs can promote generation of MDSC *in vivo* and *in vitro*, thereby protecting islet allografts against immune cell attack.[12] MDSC can also increase IL-10 production after cell-cell contact with macrophages of tumor-bearing mice.[25] These studies support our results that infiltrated BMC in fibrotic liver express the same makers as MDSC, and they further increase IL-10 expression after interacting with activated HSCs. In addition, we found an increased population of $CD4^+CD25^+Foxp3^+$ Tregs originating from recipient mice after infusion of BMC that are also anti-inflammatory based on their production of IL-10 and TGF-β (Fig. 2B).[15, 18] According to recent studies, MDSC of patients and mice with tumors contribute to the induction of Tregs.[13, 14, 17, 26] Treg induction also requires IL-10 and TGF-β of MDSCs,[14] which preferentially induces proliferation of natural Tregs[26] leading to reduced activation of macrophages and T cells. In our study, enhanced IL-10 production of infused BMC decreased the population of macrophages (Fig. 2C and Supporting Fig. 2D) and expanded Tregs in liver MNCs of recipient mice, which was reversed in recipient mice after infusion of IL-10-deficient BMC (Fig. 6D–F).

According to the previous studies, TGF-β, IL-6 and retinoic acid are not only important factors in T cell differentiation[8] but also in the activation and further differentiation of MDSC into macrophage, dendritic cells and granulocytes.[14, 19–21] Intriguingly, HSCs can produce a variety of mediators including TGF-β, IL-6 and retinoic acid depending on their state of activation.[5] Thus, in order to clarify which mediators of HSCs play an important role in BMC production of IL-10, we co-cultured BMC with HSCs deficient in the production of IL-10, IL-6 and RALDH1 or WT HSCs (Fig. 7A, B). Surprisingly, IL-6-deficient HSCs induced more IL-10 expression by BMC, whereas RALDH1-deficient HSCs had decreased IL-10 compared with that of BMC co-cultured with WT HSCs. Moreover, RALDH1-deficient mice displayed decreased production of retinoic acid[27], and did not show any anti-fibrotic effects of infused WT BMC (Fig. 7C, D and Supporting Fig. 6A). However, IL-10-deficient HSCs did not affect production of IL-10 by WT BMC. Thus, retinoic acid metabolized from retinol by RALDH1 and IL-6 in HSCs might play important roles in IL-10 production by BMC. In support of this prospect, treatment with retinoic acid increased IL-10 production in several cell lines, possibly because the IL-10 locus harbors at least one retinoic acid-response element.[28] In addition, the antagonist effect of retinoic acid on IL-6 has previously been demonstrated during T cell differentiation.[8] However the underlying mechanism is not clear. Therefore, further studies are necessary to understand the roles of IL-6 and retinoic acid in the production of IL-10 in BMC.

Recently, intriguing studies suggest that different subsets of macrophages and dendritic cells have varying roles in liver injury, fibrosis and tumor development. For instance, delivery of bone marrow-derived macrophages differentiated by colony stimulating factor-1 are reportedly beneficial by reducing fibrosis, mainly by recruiting endogenous macrophages and neutrophils producing matrix metalloproteinase (MMP)-9 and MMP-13; however, this protective effect was not detected in treatment of macrophage precursors.[29] In our study, MMP-9 and MMP-13 were increased in isolated liver MNCs from both WT and IL-10-deficient BMC-treated mice, compared to those of controls (Supporting Fig. 7B, C). Thus, the expression of MMPs was not a critical determinant of the findings in our study. In addition, dendritic cells can reduce liver ischemia/reperfusion injury and fibrosis via IL-10 secretion and MMP-9 expression respectively.[30, 31] In contrast, CD11b$^+$F4/80$^+$Gr1$^+$ macrophages promote liver fibrosis and tumor development in a TGF-β-dependant manner.[32, 33] These reports also demonstrate that various types of bone marrow-derived cells acquire different functions during liver injury. Thus, further studies to characterize functional subsets of bone marrow-derived cells should be pursued.

In summary, here we provide evidence in mice and humans that IL-10 production by infused BMC is a key negative regulator of liver fibrosis at early time points. Crucially, the interplay between HSCs and BMC is necessary for the induction of IL-10 in infused BMC (CD11b$^+$Gr1$^+$F4/80$^+$ and CD11b$^+$Gr1^{high}F4/80$^-$ MDSC-like cells), which in turn expand the Treg population in recipient mice. Our findings may contribute to the refinement of autologous BMC therapeutic approaches for patients with liver fibrosis and cirrhosis.

Supplementary Material

Refer to Web version on PubMed Central for supplementary material.

Acknowledgments

List of Abbreviations

BMC	bone marrow cells
ECM	extracellular matrix
HSC	hepatic stellate cells
TGF-β	transforming growth factor-beta
IL	interleukin
Tregs	regulatory T cells
NK cell	natural killer cell
MDSC	myeloid-derived suppressor cell
IFN	interferon
GFP	green fluorescence protein
RALDH	retinaldehyde dehydrogenase
CCl$_4$	carbon tetrachloride
α-SMA	α-smooth muscle actin
qRT-PCR	quantitative reverse-transcription polymerase chain reaction
MCP	monocyte chemoattractant protein
MNC	mononuclear cell
FACS	fluorescence-activated cell sorting
COL1A1	type 1 collagen alpha 1
WT	wild type
MMP	matrix metalloproteinase

References

1. Petersen BE, Bowen WC, Patrene KD, Mars WM, Sullivan AK, Murase N, et al. Bone marrow as a potential source of hepatic oval cells. Science. 1999; 284:1168–1170. [PubMed: 10325227]

2. Sakaida I, Terai S, Yamamoto N, Aoyama K, Ishikawa T, Nishina H, et al. Transplantation of bone marrow cells reduces CCl4-induced liver fibrosis in mice. Hepatology. 2004; 40:1304–1311. [PubMed: 15565662]

3. Terai S, Ishikawa T, Omori K, Aoyama K, Marumoto Y, Urata Y, et al. Improved liver function in patients with liver cirrhosis after autologous bone marrow cell infusion therapy. Stem Cells. 2006; 24:2292–2298. [PubMed: 16778155]

4. Biermann H, Pietz B, Dreier R, Schmid KW, Sorg C, Sunderkotter C. Murine leukocytes with ring-shaped nuclei include granulocytes, monocytes, and their precursors. J Leukoc Biol. 1999; 65:217–231. [PubMed: 10088605]

5. Hernandez-Gea V, Friedman SL. Pathogenesis of liver fibrosis. Annu Rev Pathol. 2011; 6:425–456. [PubMed: 21073339]

6. Thompson K, Maltby J, Fallowfield J, McAulay M, Millward-Sadler H, Sheron N. Interleukin-10 expression and function in experimental murine liver inflammation and fibrosis. Hepatology. 1998; 28:1597–1606. [PubMed: 9828224]

7. Radaeva S, Wang L, Radaev S, Jeong WI, Park O, Gao B. Retinoic acid signaling sensitizes hepatic stellate cells to NK cell killing via upregulation of NK cell activating ligand RAE1. Am J Physiol Gastrointest Liver Physiol. 2007; 293:G809–816. [PubMed: 17673545]

8. Mucida D, Park Y, Kim G, Turovskaya O, Scott I, Kronenberg M, et al. Reciprocal TH17 and regulatory T cell differentiation mediated by retinoic acid. Science. 2007; 317:256–260. [PubMed: 17569825]

9. Winau F, Hegasy G, Weiskirchen R, Weber S, Cassan C, Sieling PA, et al. Ito cells are liver-resident antigen-presenting cells for activating T cell responses. Immunity. 2007; 26:117–129. [PubMed: 17239632]

10. Radaeva S, Sun R, Jaruga B, Nguyen VT, Tian Z, Gao B. Natural killer cells ameliorate liver fibrosis by killing activated stellate cells in NKG2D-dependent and tumor necrosis factor-related apoptosis-inducing ligand-dependent manners. Gastroenterology. 2006; 130:435–452. [PubMed: 16472598]

11. Ichikawa S, Mucida D, Tyznik AJ, Kronenberg M, Cheroutre H. Hepatic stellate cells function as regulatory bystanders. J Immunol. 2011; 186:5549–5555. [PubMed: 21460203]

12. Chou HS, Hsieh CC, Yang HR, Wang L, Arakawa Y, Brown K, et al. Hepatic stellate cells regulate immune response by way of induction of myeloid suppressor cells in mice. Hepatology. 2011; 53:1007–1019. [PubMed: 21374665]

13. Hoechst B, Ormandy LA, Ballmaier M, Lehner F, Kruger C, Manns MP, et al. A new population of myeloid-derived suppressor cells in hepatocellular carcinoma patients induces CD4(+)CD25(+)Foxp3(+) T cells. Gastroenterology. 2008; 135:234–243. [PubMed: 18485901]

14. Huang B, Pan PY, Li Q, Sato AI, Levy DE, Bromberg J, et al. Gr-1+CD115+ immature myeloid suppressor cells mediate the development of tumor-induced T regulatory cells and T-cell anergy in tumor-bearing host. Cancer Res. 2006; 66:1123–1131. [PubMed: 16424049]

15. Saraiva M, O'Garra A. The regulation of IL-10 production by immune cells. Nat Rev Immunol. 2010; 10:170–181. [PubMed: 20154735]

16. Terai S, Sakaida I, Yamamoto N, Omori K, Watanabe T, Ohata S, et al. An in vivo model for monitoring trans-differentiation of bone marrow cells into functional hepatocytes. J Biochem. 2003; 134:551–558. [PubMed: 14607982]

17. Gabrilovich DI, Nagaraj S. Myeloid-derived suppressor cells as regulators of the immune system. Nat Rev Immunol. 2009; 9:162–174. [PubMed: 19197294]

18. Moore KW, de Waal Malefyt R, Coffman RL, O'Garra A. Interleukin-10 and the interleukin-10 receptor. Annu Rev Immunol. 2001; 19:683–765. [PubMed: 11244051]

19. Bunt SK, Yang L, Sinha P, Clements VK, Leips J, Ostrand-Rosenberg S. Reduced inflammation in the tumor microenvironment delays the accumulation of myeloid-derived suppressor cells and limits tumor progression. Cancer Res. 2007; 67:10019–10026. [PubMed: 17942936]

20. Gabrilovich DI, Velders MP, Sotomayor EM, Kast WM. Mechanism of immune dysfunction in cancer mediated by immature Gr-1+ myeloid cells. J Immunol. 2001; 166:5398–5406. [PubMed: 11313376]

21. Kusmartsev S, Cheng F, Yu B, Nefedova Y, Sotomayor E, Lush R, et al. All-trans-retinoic acid eliminates immature myeloid cells from tumor-bearing mice and improves the effect of vaccination. Cancer Res. 2003; 63:4441–4449. [PubMed: 12907617]

22. Higashiyama R, Moro T, Nakao S, Mikami K, Fukumitsu H, Ueda Y, et al. Negligible contribution of bone marrow-derived cells to collagen production during hepatic fibrogenesis in mice. Gastroenterology. 2009; 137:1459–1466. e1451. [PubMed: 19596008]

23. Si Y, Tsou CL, Croft K, Charo IF. CCR2 mediates hematopoietic stem and progenitor cell trafficking to sites of inflammation in mice. J Clin Invest. 2010; 120:1192–1203. [PubMed: 20234092]

24. Ito A, Suganami T, Yamauchi A, Degawa-Yamauchi M, Tanaka M, Kouyama R, et al. Role of CC chemokine receptor 2 in bone marrow cells in the recruitment of macrophages into obese adipose tissue. J Biol Chem. 2008; 283:35715–35723. [PubMed: 18977759]

25. Sinha P, Clements VK, Bunt SK, Albelda SM, Ostrand-Rosenberg S. Cross-talk between myeloid-derived suppressor cells and macrophages subverts tumor immunity toward a type 2 response. J Immunol. 2007; 179:977–983. [PubMed: 17617589]

26. Serafini P, Mgebroff S, Noonan K, Borrello I. Myeloid-derived suppressor cells promote cross-tolerance in B-cell lymphoma by expanding regulatory T cells. Cancer Res. 2008; 68:5439–5449. [PubMed: 18593947]

27. Ziouzenkova O, Orasanu G, Sharlach M, Akiyama TE, Berger JP, Viereck J, et al. Retinaldehyde represses adipogenesis and diet-induced obesity. Nat Med. 2007; 13:695–702. [PubMed: 17529981]

28. Tavera-Mendoza L, Wang TT, Lallemant B, Zhang R, Nagai Y, Bourdeau V, et al. Convergence of vitamin D and retinoic acid signalling at a common hormone response element. EMBO Rep. 2006; 7:180–185. [PubMed: 16322758]

29. Thomas JA, Pope C, Wojtacha D, Robson AJ, Gordon-Walker TT, Hartland S, et al. Macrophage therapy for murine liver fibrosis recruits host effector cells improving fibrosis, regeneration, and function. Hepatology. 2011; 53:2003–2015. [PubMed: 21433043]

30. Bamboat ZM, Ocuin LM, Balachandran VP, Obaid H, Plitas G, DeMatteo RP. Conventional DCs reduce liver ischemia/reperfusion injury in mice via IL-10 secretion. J Clin Invest. 2010; 120:559–569. [PubMed: 20093775]

31. Jiao J, Sastre D, Isabel Fiel M, Lee UE, Ghiassi-Nejad Z, Ginhoux F, et al. Dendritic cell regulation of carbon tetrachloride-induced murine liver fibrosis regression. Hepatology. 2011

32. Karlmark KR, Weiskirchen R, Zimmermann HW, Gassler N, Ginhoux F, Weber C, et al. Hepatic recruitment of the inflammatory Gr1+ monocyte subset upon liver injury promotes hepatic fibrosis. Hepatology. 2009; 50:261–274. [PubMed: 19554540]

33. Schiechl G, Bauer B, Fuss I, Lang SA, Moser C, Ruemmele P, et al. Tumor development in murine ulcerative colitis depends on MyD88 signaling of colonic F4/80+CD11b(high)Gr1(low) macrophages. J Clin Invest. 2011; 121:1692–1708. [PubMed: 21519141]
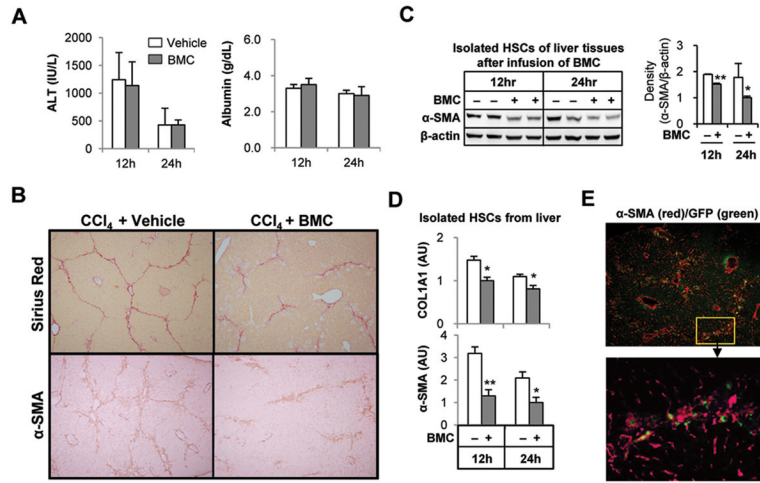
Fig. 1.
Infused BMC ameliorates CCl$_4$-induced liver fibrosis in mice. Mice with 2-week CCl$_4$–induced liver fibrosis were sacrificed at 12 or 24 hours after infusion of BMC of GFP$^+$ mice via tail vein. (A) Serum chemistry was conducted for ALT and albumin. (B) Representative Sirius red or α-SMA staining of liver tissue at 24 hours after BMC infusion (original magnification, ×100). (C) Isolated HSCs of liver tissues were subjected to Western blotting. (D) α-SMA and COL1A1 mRNA levels in isolated HSCs were determined by quantitative RT-PCR (qRT-PCR). (E) After staining with α-SMA antibody, frozen liver sections were observed under the fluorescent microscopy (original magnification, upper panels ×100; lower panels ×400). Data are expressed as the mean ± SEM (at least 8 ~ 12 mice per group). *$P < 0.05$, **$P < 0.01$ in comparison with the corresponding controls.
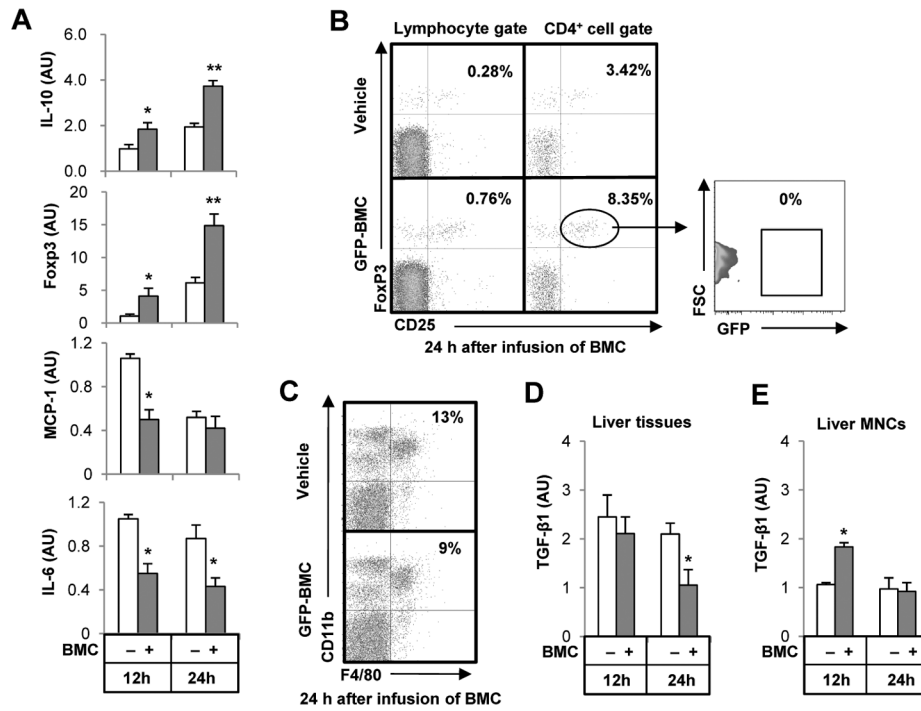
Fig. 2.
Infused BMC increase IL-10 expression and CD4^{+}CD25^{+}Foxp3^{+} Treg while decreasing the expression of IL-6 and MCP-1, and reducing F4/80^{+}CD11b^{+} cells in fibrotic liver. Mice with 2-weeks of CCl$_4$–induced liver fibrosis were sacrificed at 12 or 24 hours after infusion of BMC of GFP^{+} mice via tail vein, and then liver MNCs and tissues were isolated or collected. (A) Isolated liver MNCs were subjected to qRT-PCR. (B, C) CD4^{+}CD25^{+}Foxp3^{+} Tregs and F4/80^{+}CD11b^{+} macrophages in liver MNCs were analyzed at 24 hour after infusion of BMC. (D, E) TGF-β1 mRNA levels of whole liver tissues and isolated liver MNCs were determined by qRT-PCR. Data are expressed as the mean ± SEM (at least 8 mice per group). *$P < 0.05$, **$P < 0.01$ in comparison with the corresponding controls.
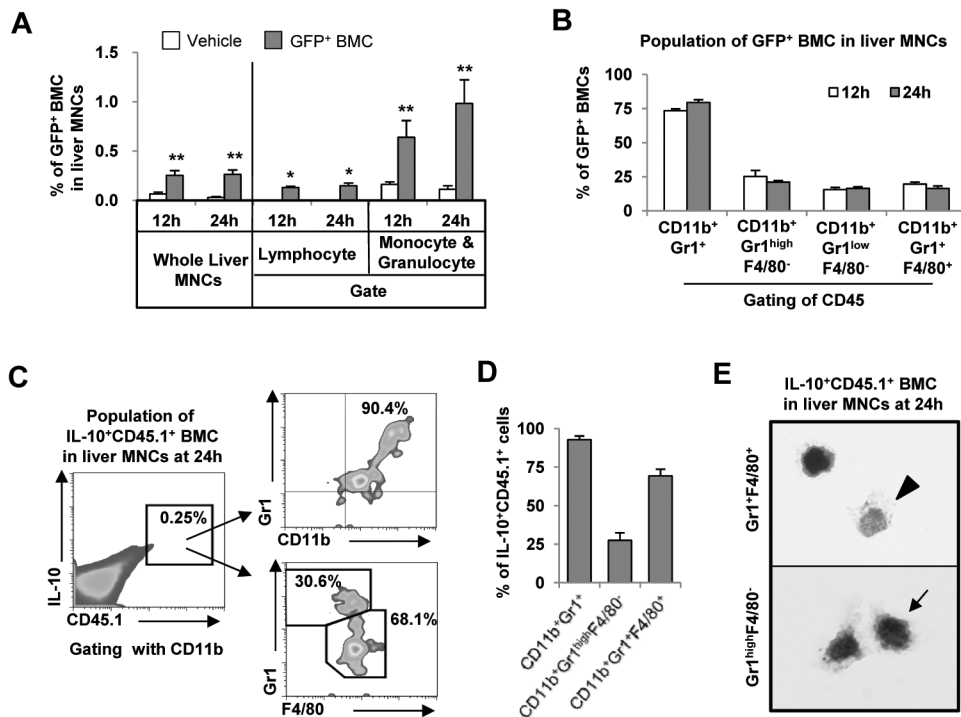
A

B Population of GFP⁺ BMC in liver MNCs

C Population of IL-10⁺CD45.1⁺ BMC in liver MNCs at 24h — Gating with CD11b

D

E IL-10⁺CD45.1⁺ BMC in liver MNCs at 24h

Fig. 3.
Infused BMC subtypes CD11b$^+$Gr1$^+$F4/80$^+$ and CD11b$^+$Gr1^{high}F4/80$^-$ play important roles in IL-10 production in fibrotic livers of recipient mice. Mice with 2-week CCl$_4$–induced liver fibrosis were sacrificed at 12 or 24 hours after infusion of BMC of GFP$^+$ or CD45.1$^+$ mice via tail vein. Liver MNCs were isolated and subjected to FACS analyses. (A) The percentages of infused BMC (GFP$^+$) to total liver MNCs were analyzed. (B) The cellular markers of GFP$^+$ BMC were analyzed using antibodies to CD45, CD11b, Gr1 and F4/80. (C, D) Intracellular cytokine staining of IL-10 was performed and analyzed for IL-10$^+$CD45.1$^+$ BMC of isolate liver MNCs. (E) Among IL-10$^+$CD45.1$^+$ BMC of isolate liver MNCs, CD11b$^+$Gr1$^+$F4/80$^+$ and CD11b$^+$Gr1^{high}F4/80$^-$ BMCs were sorted and stained with Giemsa respectively (Original magnification, ×2000). Data are expressed as the mean ± SEM (at least 5 ~ 10 mice per group). *P< 0.05, **P< 0.01 in comparison with the corresponding controls.
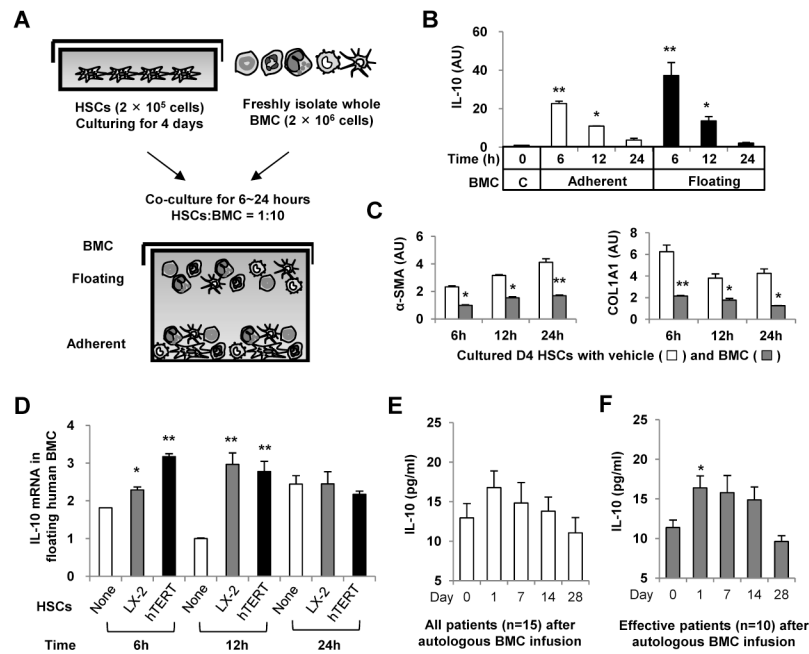
Fig. 4.
Co-culturing with HSCs enhances IL-10 expression by BMC, which suppresses activation of D4 HSCs. (A) Isolated HSCs from healthy mice were cultured on plastic dish for 4 days (D4 HSCs). Then freshly isolated BMC were co-cultured with activated D4 HSCs for 6 to 24 hours (HSCs:BMC = 1:10). (B) IL-10 mRNA levels in adherent and floating BMC of mice were determined by qRT-PCR. (C) After co-culturing, α-SMA and COL1A1 mRNA levels of D4 HSCs of mice were determined by qRT-PCR. (D) Human HSCs (LX-2 and hTERT cell lines) were co-cultured with human BMC of HBV patients for 6 to 24 hours after 6 hour-starvation of human HSCs. IL-10 mRNA levels in floating human BMC were determined by qRT-PCR. (E) IL-10 levels of sera in HBV patients (n=15) with cirrhosis were measured at various time points and analyzed after autologous BMC infusion. (F) After autologous BMC infusion, IL-10 levels in blood were analyzed in the effective patients (n=10) of all patients (n=15) showing the improvement of Child-Pugh scoring and albumin levels. Data are expressed as the mean ± SEM via 3 ~ 5 independent experiments. *$P < 0.05$, **$P < 0.01$ in comparison with the corresponding controls.

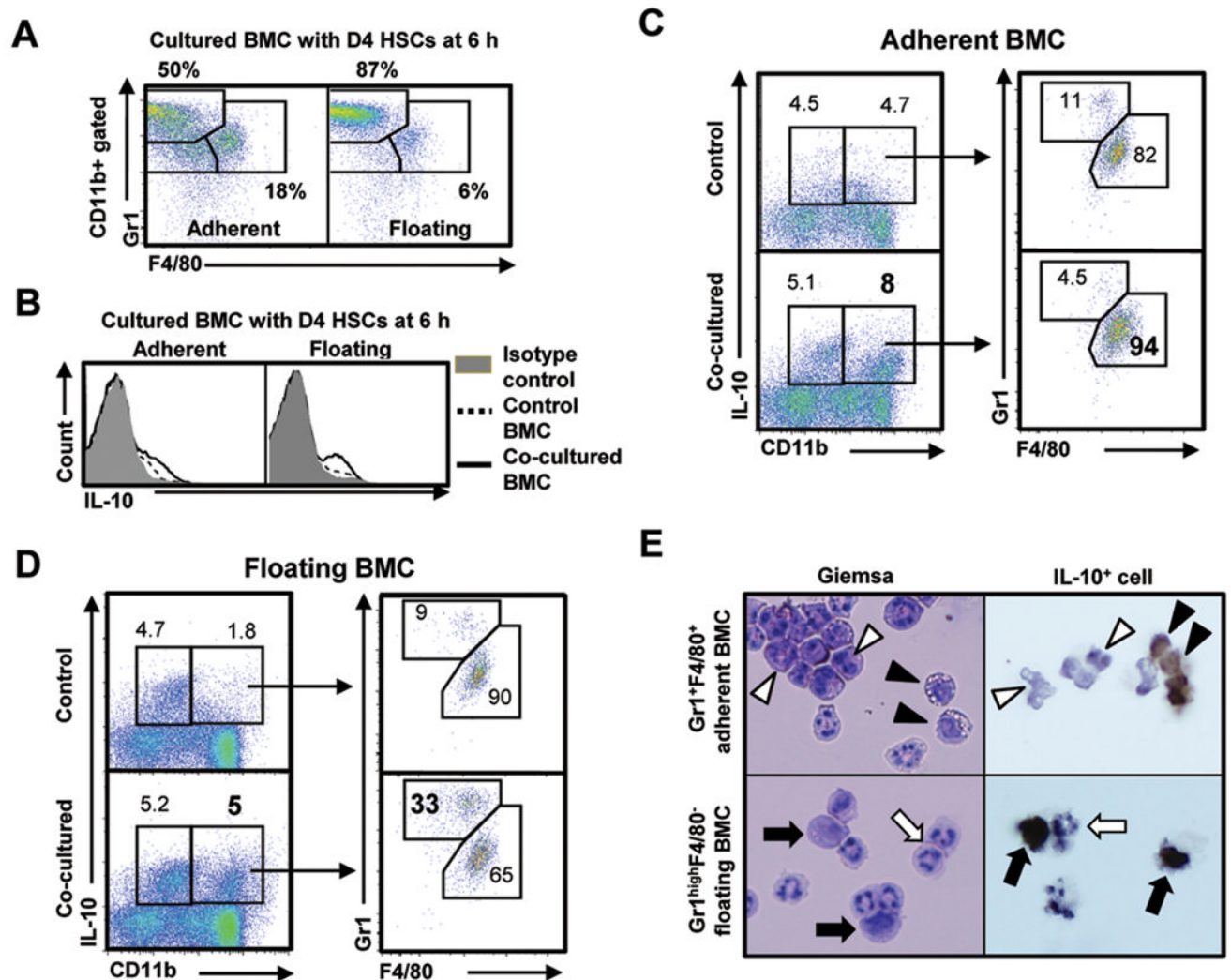**Fig. 5.**
CD11b$^+$Gr1^{high}F4/80$^-$ and CD11b$^+$Gr1$^+$F4/80$^+$ BMC enhance IL-10 expression after co-culturing with D4 HSCs. BMC isolated from normal mice were co-cultured with D4 HSCs. (A) Adherent and floating BMC were analyzed using antibodies to Gr1 and F4/80 after co-culturing with D4 HSCs for 6 hours. (B) IL-10 positive BMC increased in both adherent and floating BMC after co-culturing. (C, D) IL-10 positive BMC were analyzed using antibodies to IL-10, CD11b, Gr1 and F4/80. (E) Co-cultured BMC (CD11b$^+$Gr1^{high}F4/80$^-$ and CD11b$^+$Gr1$^+$F4/80$^+$) were sorted using FACS Aria and then stained with Giemsa or intracellular cytokine staining of IL-10 were performed after further culturing with monensin for additional 18 hours (original magnification, ×1200). IL-10 positive cells were indicated as black arrowhead or black arrow, and IL-10 negative cells were shown as white arrowhead or white arrow. Data are expressed as the mean ± SEM via 5 independent experiments. *$P < 0.05$, **$P < 0.01$ in comparison with the corresponding controls.
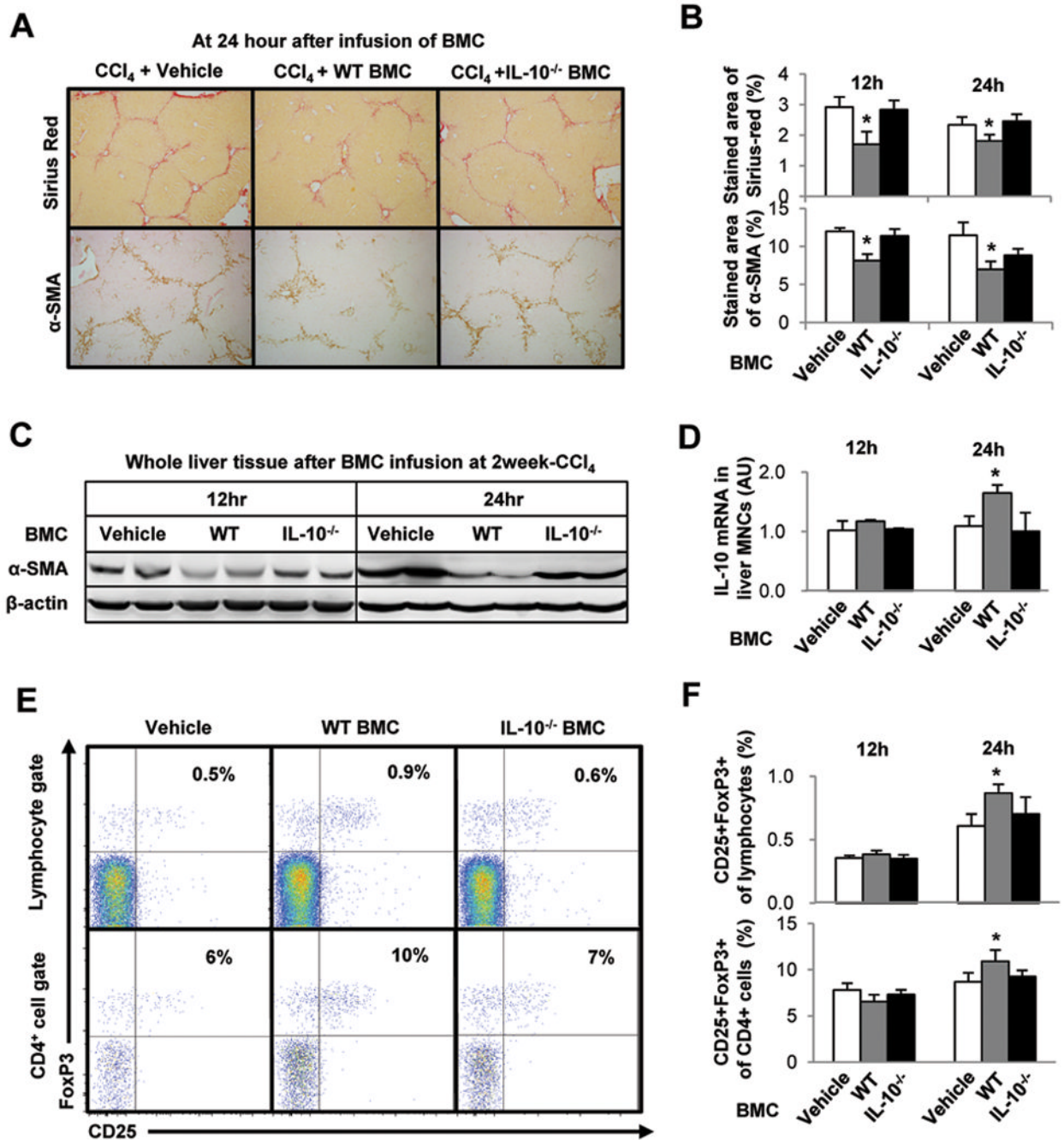
Fig. 6.
Depletion of IL-10 gene in BMC abrogates the anti-fibrotic effects of BMC via down regulation of IL-10 expression and Treg induction in liver MNCs of recipient mice. Mice with 2-week CCl$_4$-induced liver fibrosis were infused with vehicle, isolated whole BMC of control WT or IL-10$^{-/-}$ mice through tail vein. Mice were sacrificed at 12 and 24 hours after BMC infusion. (A, B) To estimate liver fibrosis and HSC activation, sections of liver tissues were stained with Sirius red and α-SMA antibody. The stained areas of Sirius red and α-SMA antibody were calculated with image analyzer program. (C) Whole liver tissues were subjected to Western blotting. (D) IL-10 mRNA levels in liver MNCs were determined qRT-PCR analyses. (E, F) Intrahepatic CD4$^+$CD25$^+$FoxP3$^+$ Treg increased in the mice

treated with WT BMC but not in IL-10$^{-/-}$ BMC at 24 hour. Data are expressed as the mean ± SEM (at least 8 ~ 10 mice per group). $*P < 0.05$ in comparison with the corresponding controls.
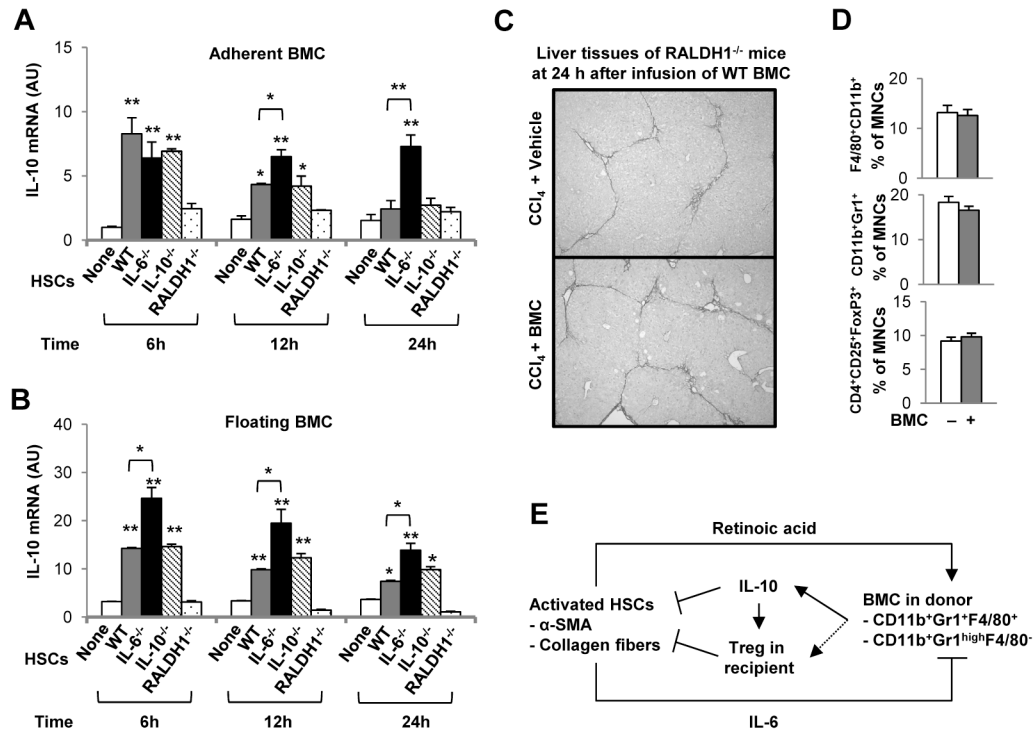
Fig. 7.
IL-10 expression of BMC is promoted or suppressed by retinoic acid and IL-6 of HSCs, respectively. Isolated HSCs from WT, IL-6$^{-/-}$, IL-10$^{-/-}$ and RALDH1$^{-/-}$ mice were cultured on plastic plates for 4 days (D4 HSCs). Then freshly isolated WT BMC from control mice were co-cultured with activated D4 HSCs for 6 to 24 hours (HSCs:BMC = 1:10) or cultured alone as control. (A, B) After co-culturing, IL-10 expressions in the adherent and floating BMC were analyzed using qRT-PCR. RALDH1$^{-/-}$ mice with 2-weekCCl$_4$-induced liver fibrosis were infused with isolated whole BMC of WT mice through tail vein and then were sacrificed at 24 h after infusion of BMC. (C) Representative Sirius red staining of liver tissue (original magnification, ×100). (D) There were no significant changes in the population of Gr1$^+$CD11b$^+$ and F4/80$^+$CD11b$^+$ cells in liver, and intrahepatic CD4$^+$CD25$^+$FoxP3$^+$ Treg did not increase in RALDH1$^{-/-}$ mice after infusion of WT BMC at 24 hours. (E) An integrated depiction of anti-fibrotic roles of infused BMC after interaction with HSCs. First, the interaction between infused BMC and HSCs is crucial for IL-10 production in infused BMC (especially CD11b$^+$Gr1$^+$F4/80$^+$ and CD11b$^+$Gr1^{high}F4/80$^-$ MDSC-like cells). Second, retinoic acid and IL-6 from activated HSCs stimulate and inhibit respectively the production of IL-10 by infused BMC. Third, IL-10 from infused BMC of donor mice is essential for the induction of Treg in recipient mice, which then suppresses activated HSCs via direct (IL-10 production) and indirect (Treg induction) effects of infused BMC. Data are expressed as the mean ± SEM via 3 independent experiments or using 8 mice per group. *$P < 0.05$, **$P < 0.01$ in comparison with the corresponding controls.